

Brief Report

Intra-Host SARS-CoV-2 Evolution in the Gut of Mucosally-Infected *Chlorocebus aethiops* (African Green Monkeys)

Lori A. Rowe ^{1,†}, Brandon J. Beddingfield ^{1,†}, Kelly Goff ¹, Stephanie Z. Killeen ¹, Nicole R. Chirichella ¹, Alexandra Melton ¹, Chad J. Roy ^{1,2} and Nicholas J. Maness ^{1,2,*}

¹ Tulane National Primate Research Center, Covington, LA 70433, USA; lrowe1@tulane.edu (L.A.R.); bbedding@tulane.edu (B.J.B.); kgoff@tulane.edu (K.G.); smoore2@tulane.edu (S.Z.K.); nchirichella@tulane.edu (N.R.C.); amelton@tulane.edu (A.M.); croy@tulane.edu (C.J.R.)

² Department of Microbiology and Immunology, Tulane University School of Medicine, New Orleans, LA 70112, USA

* Correspondence: nmaness@tulane.edu

† These authors contributed equally to this work.

Abstract: In recent months, several SARS-CoV-2 variants have emerged that enhance transmissibility and escape host humoral immunity. Hence, the tracking of viral evolutionary trajectories is clearly of great importance. Little is known about SARS-CoV-2 evolution in nonhuman primate models used to test vaccines and therapies and to model human disease. Viral RNA was sequenced from rectal swabs from *Chlorocebus aethiops* (African green monkeys) after experimental respiratory SARS-CoV-2 infection. Two distinct patterns of viral evolution were identified that were shared between all collected samples. First, mutations in the furin cleavage site that were initially present in the virus as a consequence of VeroE6 cell culture adaptation were not detected in viral RNA recovered in rectal swabs, confirming the necessity of this motif for viral infection in vivo. Three amino acid changes were also identified; ORF 1a S2103F, and spike D215G and H655Y, which were detected in rectal swabs from all sampled animals. These findings are demonstrative of intra-host SARS-CoV-2 evolution and may identify a host-adapted variant of SARS-CoV-2 that would be useful in future primate models involving SARS-CoV-2 infection.

Keywords: SARS-CoV-2; evolution; African green monkey (*Chlorocebus aethiops*)



Citation: Rowe, L.A.; Beddingfield, B.J.; Goff, K.; Killeen, S.Z.; Chirichella, N.R.; Melton, A.; Roy, C.J.; Maness, N.J. Intra-Host SARS-CoV-2 Evolution in the Gut of Mucosally-Infected *Chlorocebus aethiops* (African Green Monkeys). *Viruses* **2022**, *14*, 77. <https://doi.org/10.3390/v14010077>

Academic Editors: Mahesh Mohan and Karol Sestak

Received: 4 September 2021

Accepted: 23 December 2021

Published: 1 January 2022

Publisher's Note: MDPI stays neutral with regard to jurisdictional claims in published maps and institutional affiliations.



Copyright: © 2022 by the authors. Licensee MDPI, Basel, Switzerland. This article is an open access article distributed under the terms and conditions of the Creative Commons Attribution (CC BY) license (<https://creativecommons.org/licenses/by/4.0/>).

1. Introduction

The COVID-19 pandemic, caused by the coronavirus SARS-CoV-2, has killed more than 4 million people to date. Despite the development and rollout of safe and highly effective vaccines on an unparalleled time scale, nearly unchecked viral spread has continued due to vaccine refusal and hesitancy in nations with adequate vaccine supply coupled with inadequate supply in many regions of the world. As a result, several new variants have emerged with enhanced replicative or infectious capacity and immune escape [1]. Since the discovery of the D614G mutation [2,3], noted early in the pandemic and found to enable enhanced infection in cells and is now present in all sequenced isolates, several variants of interest and concern (as defined by the CDC) have arisen [1,4–11]. These include B.1.1.7 (alpha), which was originally detected in the United Kingdom and rapidly spread globally, B.1.351 (beta), originally detected in South Africa, and P.1 (gamma), originally detected in Japan in a traveler from Brazil. More recently, the B.1.617.2 (delta) variant rapidly became globally dominant, which is of great concern due to its greatly enhanced transmissibility relative to other variants and its ability to infect vaccinated individuals [12]. At the time of this submission, the B.1.1.529 (omicron) is rapidly increasing in frequency and may overtake delta as the globally dominant variant [13,14]. Collectively, these data suggest a

concerning scenario wherein continued SARS-CoV-2 evolution may facilitate persistence and spread in populations, including those with preexisting immunity to the virus.

Several animal species have been tested in efforts to develop a model that faithfully recapitulates human disease and associated pathological consequences, ultimately to be used in the evaluation of vaccines and therapies for COVID-19. Multiple nonhuman primate (NHP) species have been explored to this end, including *Macaca mulatta* (rhesus macaque) (RhM), *Papio anubis* (baboons) [15], *Macaca nemestrina* (pigtail macaques) [16], *Macaca fascicularis* (cynomolgus macaque), and *Chlorocebus aethiops* (African green monkeys; AGM) [17–19]. Although some data suggest enhanced disease in AGM relative to other species [17], SARS-CoV-2 replicates to high titer in all of these species. However, in most cases, viral replication in upper respiratory sites is restricted to the first several days after infection. Thus, detection of intrahost evolution in these sites may be limited. Importantly, it is now becoming clear that the virus can persist and continue to replicate in gastrointestinal sites [20,21], which provides an opportunity to examine viral evolution beyond the first several days of infection and may illuminate tissue-specific compartmentalized evolution.

We recently conducted a study to compare viral and host dynamics in RhM and AGM. Four of each species were infected via the combined intratracheal/intranasal route, and four of each were infected via aerosolized virus. All animals were euthanized four weeks after infection. Viral dynamics were largely the same regardless of route, and AGM tended, on average, to have detectable viral RNA for a longer period, including multiple animals that maintained replicating virus (as evidenced by qRT PCR detection of subgenomic viral RNA) in rectal swab samples for the entirety of the study [22]. Unfortunately, most samples from that study were exhausted and could not be used for sequencing.

In this study, a focused set of gastrointestinal samples from a previous study [22] was used to examine viral dynamics in SARS-CoV-2 infected African green monkeys (AGM). Consistent patterns of evolution were identified, suggestive of adaptive evolution. The available samples were exclusively rectal swabs, which suggest viral replication in the gastrointestinal system may be an important source of viral variants. Notably, these results have important implications for the detection of SARS-CoV-2 variants in wastewater [23,24].

2. Materials and Methods

2.1. NHP Experiments

Eight RhM and eight AGM were challenged with SARS-CoV-2, WA1/2020 isolate, as described [22]. Briefly, four of each species were challenged via the combined intratracheal/intranasal route (2×10^6 TCID₅₀) and four via aerosolized virus from the same stock. Aerosolization inherently leads to a lower effective dose, so animals challenged via this route were estimated to receive a dose between 100 and 1000 times lower than those that received direct mucosal instillation. Viral titers were quantified in several respiratory sites using primers and probes specific to the N gene (for total viral RNA) and specific for both the N and E subgenomic RNAs to approximate replicating virus.

2.2. Sample Collection, RNA Isolation and Conversion to cDNA

Rectal Swabs were collected and stored in RNA/DNA Shield (Zymo Research, Irvine, CA, USA). RNA was isolated using the Zymo Quick-RNA Viral kit and converted to cDNA using Protoscript II (New England Biolabs, Ipswich, MA, USA) as follows: 10 µL Template RNA, 1 µL 10 µM random hexamers, and 1 µL 10 mM dNTPs were incubated at 65 °C for 5 min and then placed directly on ice for 1 min. The following was then added: 4 µL PSII buffer, 2 µL 100 mM DTT, 1 µL RNase inhibitor, and 1 µL PSII reverse transcriptase and incubated at 42 °C for 50 min, then 70 °C for 10 min, followed by a hold at 4 °C.

2.3. Sequencing

DNA libraries were made using the standard SWIFT Normalase Amplicon Panels protocol (SWIFT Biosciences, Ann Arbor, MI, USA) utilizing the SNAP UD indexing primers.

The libraries were normalized to 4 nM and pooled. Paired-end sequencing (2×150) was performed on the Illumina (San Diego, CA, USA) MiSeq platform.

2.4. Data Analysis

Primer sequences were trimmed, and sequence reads were aligned to the SARS-CoV-2 genome (WA1/2020 isolate, accession MN985325) using the built-in mapping function in Geneious Prime software. Variants were called that were present at greater than 10% of reads at that site. Variants detected in the SARS-CoV-2 spike structure were visualized with UCSF Chimera, developed by the Resources for Biocomputing, Visualization, and Informatics at the University of California, San Francisco, CA, USA [25].

3. Results and Discussion

A high-density overlapping amplicon approach was used to amplify and sequence the entire SARS-CoV-2 genome from the viral stock used to experimentally infect the AGM in our previous study [23]. Rectal swabs isolated from three AGM infections at 2 or 4 weeks post-infection were analyzed in the same fashion. The challenge stock harbored several mutations of various frequencies relative to the WA1/2020 patient isolate (Figure 1A). These included two mutations in spike, F79L, and a high-frequency mutation that changed the arginine (R) at position 682 to a leucine (R682L) (Figure 1A). This residue is the second arginine and one of the key residues in the furin cleavage site, most likely the result of adaptation to VeroE6 cells. This stock was used to infect 16 NHP (8 RhM and 8 AGM). Samples were acquired from nasal, oropharyngeal, and rectal swabs from time points spanning four weeks post-infection. RNA extracted from swabs at early time points was exhausted from extensive qRT PCR characterization, and focus was shifted to rectal swabs collected from late time points, including 14 and 28 days post-infection in three of the AGMs. Sequencing of these samples revealed a consistent pattern of evolution in vivo with three mutations arising in all three animals; ORF1a/b S2103F, spike D215G, and spike H655Y (Figure 1B). In contrast, F79L and R682L mutations, present at approximately 60 and 80% in the virus stock, respectively, were completely absent in all rectal samples.

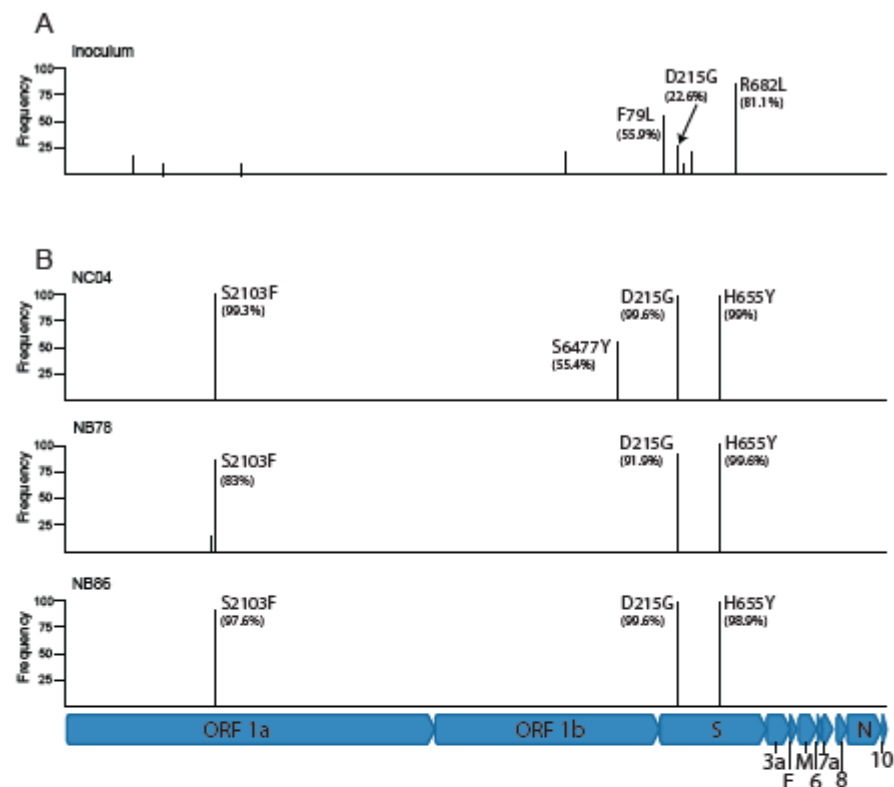


Figure 1. Cont.

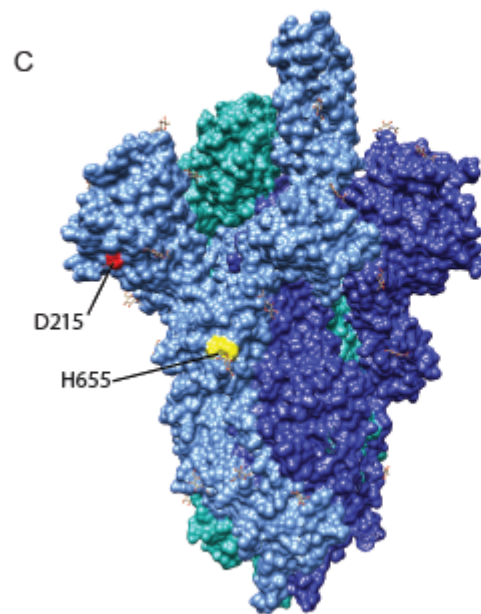


Figure 1. Viral evolution detected in rectal swabs in SARS-CoV-2 infected AGM. (A) AGMs were challenged via an intranasal and intratracheal route with SARS-CoV-2 using a stock of the WA1/2020 isolate harboring several variants relative to the patient sample. (B) Sequencing of viral RNA isolated from rectal swabs at 3–4 weeks after challenge revealed a consistent pattern of variants in all three animals. (C) Two spike mutations detected in all animals map to the N-terminal domain (D215G) and near the furin cleavage site (H655Y) based on a spike structure (PBD 7K8Z [26]).

Importantly, we note that since available samples used in this report were solely from rectal swabs and solely from AGM, we cannot draw conclusions regarding whether the mutations we identified are specific to this compartment or to this species. Our data simply provide evidence that ongoing viral replication in this compartment can lead to the accumulation of viral mutations, which has not been noted in animal models of COVID-19. More work will be necessary to assess whether these or other mutations occur in respiratory sites, which would be critical for viral transmission.

The ORF1a/b residue 2103 lies in nonstructural protein 3 (nsp3), which is the largest protein in the SARS-CoV-2 proteome and localizes with other viral proteins to the cell membrane [27,28]. The S2103F mutation in this protein has been detected at low frequency in human samples, including in India [29], but is not restricted to a particular clade and, through the course of the pandemic, has never been detected in greater than 1% of all sequenced isolates (nextstrain.org accessed on 29 November 2021 [30,31]).

The loss of the F79L mutation, present at a relatively low frequency in the inoculum and lost *in vivo*, may simply reflect the outgrowth of viral variants containing the wild type residue at this position rather than selection. However, the R682L mutation has been noted before in stocks of this virus expanded in Vero E6 cells [32,33] and likely eliminates the furin cleavage site in spike. Reversion to the wild-type amino acid, therefore, likely confirms the necessity of the furin cleavage site for infection *in vivo*, which has been previously suggested [34]. This finding, although not unexpected, confirms that the loss of the furin cleavage site *in vitro* can be ascribed to replication in VeroE6 cells [35]. Since VeroE6 cells are sourced from AGM kidneys, this finding confirms the loss of the furin cleavage site to be an *in vitro* phenomenon and not specific to replication in AGM cells *per se*. The D215G mutation rose from approximately 15% prevalence in the stock to near 100% in all three animals. This mutation lies in the N-terminal domain of the spike protein (Figure 1C) and is detected at low frequency in multiple viral lineages and is a defining variant of the B.1.351 (beta) lineage (nextstrain.org). One report showed this mutation has

a weak but detectable impact on augmenting cell to cell fusion [36]. The H655Y mutation lies immediately adjacent to the furin cleavage site (Figure 1C) and has been detected in multiple viral lineages, with the P.1 (gamma) and B.1.1.529 (omicron) lineages being most prominent (nextstrain.org). This variant has also been detected in other animal species disease models, including cats and mink [37,38]. A recent report also showed that virus harboring a 655Y amino acid showed enhanced replicative capacity in vitro and spike protein cleavage [38], likely explaining the H655Y mutation in the AGM species.

In this study, we define a consistent pattern of viral evolution in SARS-CoV-2-infected AGM. Despite a limited sample size, the ubiquity with which this pattern was detected strongly suggests a selective advantage to the identified mutations. All samples used in this study were derived from rectal rather than respiratory samples, and the data do not clearly suggest a possible mechanism for this selection. It is plausible that replication in the GI tract presents a unique set of selective forces on the virus driving evolution to the mutations identified. Long-term persistence of the virus in the gastrointestinal tract, as has been suggested for SARS-CoV-2 in humans and is a well-described phenomenon in other coronaviruses [39], may also allow selected mutations to accumulate. Even in the latter case, these data suggest the virus continues to replicate and evolve throughout the gastrointestinal system, which may further reveal novel aspects of the virus-host relationship and may have important implications for the detection of variants in wastewater.

4. Conclusions

These data and study support two important conclusions. First, previous reports that an intact furin cleavage site is important for infection in vivo were confirmed in this study. Second, the combination of the three mutations identified (ORF1a/b S2103F, spike D215G, and spike H655Y) may represent an adaptation to AGM or to NHP generally. Future experiments may include infection of AGM (or other nonhuman primate species) with this virus to assess the possible enhancement of pathogenesis and to optimize infectious challenges in product evaluation studies.

Author Contributions: L.A.R., B.J.B., C.J.R. and N.J.M. conceived and designed the experiments. L.A.R., B.J.B., K.G., S.Z.K., N.R.C. and A.M. performed the experiments and assisted with sample manipulation. N.J.M. and C.J.R. drafted the manuscript. All authors have read and agreed to the published version of the manuscript.

Funding: This work was supported by NIH/NIAID contract HHSN27220170033I (CJR) and grant P51OD01110459, the TNPRC base grant.

Institutional Review Board Statement: The use of nonhuman primates in this project was reviewed and approved by the Tulane Institutional Animal Care and Use Committee (IACUC), protocol P0447.

Data Availability Statement: Sequence data obtained in this study are available on the Global Initiative on Sharing All Influenza Data (GISAID) database under accession numbers EPI_ISL_8207137, EPI_ISL_8207138, EPI_ISL_8207139, and EPI_ISL_8207140.

Conflicts of Interest: The authors declare no conflict of interest.

References

1. Winger, A.; Caspari, T. The Spike of Concern-The Novel Variants of SARS-CoV-2. *Viruses* **2021**, *13*, 1002. [[CrossRef](#)] [[PubMed](#)]
2. Zhang, L.; Jackson, C.B.; Mou, H.; Ojha, A.; Peng, H.; Quinlan, B.D.; Rangarajan, E.S.; Pan, A.; Vanderheiden, A.; Suthar, M.S.; et al. SARS-CoV-2 spike-protein D614G mutation increases virion spike density and infectivity. *Nat. Commun.* **2020**, *11*, 1–9. [[CrossRef](#)]
3. Korber, B.; Fischer, W.M.; Gnanakaran, S.; Yoon, H.; Theiler, J.; Abfalterer, W.; Hengartner, N.; Giorgi, E.E.; Bhattacharya, T.; Foley, B.; et al. Tracking Changes in SARS-CoV-2 Spike: Evidence that D614G Increases Infectivity of the COVID-19 Virus. *Cell* **2020**, *182*, 812–827.e19. [[CrossRef](#)]
4. Chen, R.E.; Zhang, X.; Case, J.B.; Winkler, E.S.; Liu, Y.; VanBlargan, L.A.; Liu, J.; Errico, J.M.; Xie, X.; Suryadevara, N.; et al. Resistance of SARS-CoV-2 variants to neutralization by monoclonal and serum-derived polyclonal antibodies. *Nat. Med.* **2021**. [[CrossRef](#)] [[PubMed](#)]

5. Vidal, S.J.; Collier, A.Y.; Yu, J.; McMahan, K.; Tostanoski, L.H.; Ventura, J.D.; Aid, M.; Peter, L.; Jacob-Dolan, C.; Anioke, T.; et al. Correlates of Neutralization Against SARS-CoV-2 Variants of Concern by Early Pandemic Sera. *J. Virol.* **2021**, *95*. [[CrossRef](#)]
6. Janik, E.; Niemcewicz, M.; Podogrocki, M.; Majsterek, I.; Bijak, M. The Emerging Concern and Interest SARS-CoV-2 Variants. *Pathogens* **2021**, *10*, 633. [[CrossRef](#)]
7. Akkiz, H. Implications of the Novel Mutations in the SARS-CoV-2 Genome for Transmission, Disease Severity, and the Vaccine Development. *Front. Med.* **2021**, *8*, 636532. [[CrossRef](#)] [[PubMed](#)]
8. Focosi, D.; Maggi, F. Neutralising antibody escape of SARS-CoV-2 spike protein: Risk assessment for antibody-based Covid-19 therapeutics and vaccines. *Rev. Med. Virol.* **2021**, *31*. [[CrossRef](#)]
9. Geers, D.; Shamier, M.C.; Bogers, S.; den Hartog, G.; Gommers, L.; Nieuwkoop, N.N.; Schmitz, K.S.; Rijsbergen, L.C.; van Osch, J.A.T.; Dijkhuizen, E.; et al. SARS-CoV-2 variants of concern partially escape humoral but not T-cell responses in COVID-19 convalescent donors and vaccinees. *Sci. Immunol.* **2021**, *6*, eabj1750. [[CrossRef](#)]
10. McCallum, M.; De Marco, A.; Lempp, F.A.; Tortorici, M.A.; Pinto, D.; Walls, A.C.; Beltramello, M.; Chen, A.; Liu, Z.; Zatta, F.; et al. N-terminal domain antigenic mapping reveals a site of vulnerability for SARS-CoV-2. *Cell* **2021**, *184*, 2332–2347.e16. [[CrossRef](#)]
11. Martin, D.P.; Weaver, S.; Tegally, H.; San, J.E.; Shank, S.D.; Wilkinson, E.; Lucaci, A.G.; Giandhari, J.; Naidoo, S.; Pillay, Y.; et al. The emergence and ongoing convergent evolution of the SARS-CoV-2 N501Y lineages. *Cell* **2021**, *184*. [[CrossRef](#)] [[PubMed](#)]
12. Puranik, A.; Lenehan, P.J.; Silvert, E.; Niesen, M.J.M.; Corchado-Garcia, J.; O'horo, J.C.; Virk, A.; Swift, M.D.; Halamka, J.; Badley, A.D.; et al. Comparison of two highly-effective mRNA vaccines for COVID-19 during periods of Alpha and Delta variant prevalence. *medRxiv* **2021**. [[CrossRef](#)]
13. CDC COVID-19 Response Team. SARS-CoV-2 B.1.1.529 (Omicron) Variant—United States, 1–8 December 2021. *MMWR. Morb. Mortal. Wkly. Rep.* **2021**, *70*, 1731–1734. [[CrossRef](#)] [[PubMed](#)]
14. Cele, S.; Jackson, L.; Khan, K.; Khoury, D.S.; Moyo-Gwete, T.; Tegally, H.; Scheepers, C.; Amoako, D.; Karim, F.; Bernstein, M.; et al. SARS-CoV-2 Omicron has extensive but incomplete escape of Pfizer BNT162b2 elicited neutralization and requires ACE2 for infection. *medRxiv* **2021**. [[CrossRef](#)]
15. Singh, D.K.; Singh, B.; Ganatra, S.R.; Gazi, M.; Cole, J.; Thippeshappa, R.; Alfson, K.J.; Clemmons, E.; Gonzalez, O.; Escobedo, R.; et al. Responses to acute infection with SARS-CoV-2 in the lungs of rhesus macaques, baboons and marmosets. *Nat. Microbiol.* **2021**, *6*, 73–86. [[CrossRef](#)] [[PubMed](#)]
16. Melton, A.; Doyle-Meyers, L.A.; Blair, R.V.; Midkiff, C.; Melton, H.J.; Russell-Lodrigue, K.; Aye, P.P.; Schiro, F.; Fahlberg, M.; Szeltner, D.; et al. The pigtail macaque (*Macaca nemestrina*) model of COVID-19 reproduces diverse clinical outcomes and reveals new and complex signatures of disease. *PLoS Pathog.* **2021**, *17*, e1010162. [[CrossRef](#)] [[PubMed](#)]
17. Blair, R.V.; Vaccari, M.; Doyle-Meyers, L.A.; Roy, C.J.; Russell-Lodrigue, K.; Fahlberg, M.; Monjure, C.J.; Beddingfield, B.; Plante, K.S.; Plante, J.A.; et al. Acute Respiratory Distress in Aged, SARS-CoV-2-Infected African Green Monkeys but Not Rhesus Macaques. *Am. J. Pathol.* **2020**, *191*, 274–282. [[CrossRef](#)] [[PubMed](#)]
18. Munster, V.J.; Feldmann, F.; Williamson, B.N.; van Doremalen, N.; Perez-Perez, L.; Schulz, J.; Meade-White, K.; Okumura, A.; Callison, J.; Brumbaugh, B.; et al. Respiratory disease in rhesus macaques inoculated with SARS-CoV-2. *Nature* **2020**, *585*, 268–272. [[CrossRef](#)] [[PubMed](#)]
19. Finch, C.L.; Crozier, I.; Lee, J.H.; Byrum, R.; Cooper, T.K.; Liang, J.; Sharer, K.; Solomon, J.; Sayre, P.J.; Kocher, G.; et al. Characteristic and quantifiable COVID-19-like abnormalities in CT- and PET/CT-imaged lungs of SARS-CoV-2-infected crab-eating macaques (*Macaca fascicularis*). *bioRxiv* **2020**. [[CrossRef](#)]
20. Gaebler, C.; Wang, Z.; Lorenzi, J.C.C.; Muecksch, F.; Finkin, S.; Tokuyama, M.; Cho, A.; Jankovic, M.; Schaefer-Babajew, D.; Oliveira, T.Y.; et al. Evolution of antibody immunity to SARS-CoV-2. *Nature* **2021**, *591*, 639–644. [[CrossRef](#)]
21. Hartman, A.L.; Nambulli, S.; McMillen, C.M.; White, A.G.; Tilston-Lunel, N.L.; Albe, J.R.; Cottle, E.; Dunn, M.D.; James Frye, L.; Gilliland, T.H.; et al. SARS-CoV-2 infection of African green monkeys results in mild respiratory disease discernible by PET/CT imaging and shedding of infectious virus from both respiratory and gastrointestinal tracts. *PLoS Pathog.* **2020**, *16*, e1008903. [[CrossRef](#)] [[PubMed](#)]
22. Fears, A.C.; Beddingfield, B.J.; Chirichella, N.R.; Slisarenko, N.; Killeen, S.Z.; Redmann, R.K.; Goff, K.; Spencer, S.; Picou, B.; Golden, N.; et al. Myeloid cell-driven nonregenerative pulmonary scarring is conserved in multiple 1 nonhuman primate species regardless of SARS-CoV-2 infection modality. *bioRxiv* **2021**. [[CrossRef](#)]
23. Wannigama, D.L.; Amarasiri, M.; Hurst, C.; Phattharapornjaroen, P.; Abe, S.; Hongsing, P.; Rad, S.; Pearson, L.; Saethang, T.; Luk-In, S.; et al. Tracking COVID-19 with wastewater to understand asymptomatic transmission. *Int. J. Infect. Dis.* **2021**, *108*, 296–299. [[CrossRef](#)]
24. Mishra, S.; Mindermann, S.; Sharma, M.; Whittaker, C.; Mellan, T.A.; Wilton, T.; Klapsa, D.; Mate, R.; Fritzsche, M.; Zambon, M.; et al. Changing composition of SARS-CoV-2 lineages and rise of Delta variant in England. *EClinicalMedicine* **2021**, *39*, 101064. [[CrossRef](#)]
25. Pettersen, E.F.; Goddard, T.D.; Huang, C.C.; Couch, G.S.; Greenblatt, D.M.; Meng, E.C.; Ferrin, T.E. UCSF Chimera—A visualization system for exploratory research and analysis. *J. Comput. Chem.* **2004**, *25*, 1605–1612. [[CrossRef](#)]
26. Barnes, C.O.; Jette, C.A.; Abernathy, M.E.; Dam, K.A.; Esswein, S.R.; Gristick, H.B.; Malyutin, A.G.; Sharaf, N.G.; Huey-Tubman, K.E.; Lee, Y.E.; et al. SARS-CoV-2 neutralizing antibody structures inform therapeutic strategies. *Nature* **2020**, *588*, 682–687. [[CrossRef](#)] [[PubMed](#)]

27. Neuman, B.W.; Joseph, J.S.; Saikatendu, K.S.; Serrano, P.; Chatterjee, A.; Johnson, M.A.; Liao, L.; Klaus, J.P.; Yates, J.R.; Wüthrich, K.; et al. Proteomics Analysis Unravels the Functional Repertoire of Coronavirus Nonstructural Protein 3. *J. Virol.* **2008**, *82*, 5279–5294. [[CrossRef](#)]
28. Lei, J.; Kusov, Y.; Hilgenfeld, R. Nsp3 of coronaviruses: Structures and functions of a large multi-domain protein. *Antivir. Res.* **2017**, *149*, 58–74. [[CrossRef](#)] [[PubMed](#)]
29. Roy, S.; Nath, H.; Mallick, A.; Biswas, S. SARS-CoV-2 has observably higher propensity to accept uracil as nucleotide 1 substitution: Prevalence of amino acid substitutions and their predicted functional 2 implications in circulating SARS-CoV-2 in India up to. *bioRxiv* **2020**. [[CrossRef](#)]
30. Sagulenko, P.; Puller, V.; Neher, R.A. TreeTime: Maximum-likelihood phylodynamic analysis. *Virus Evol.* **2018**, *4*, vex042. [[CrossRef](#)]
31. Hadfield, J.; Megill, C.; Bell, S.M.; Huddleston, J.; Potter, B.; Callender, C.; Sagulenko, P.; Bedford, T.; Neher, R.A. Nextstrain: Real-time tracking of pathogen evolution. *Bioinformatics* **2018**, *34*, 4121–4123. [[CrossRef](#)] [[PubMed](#)]
32. Lamers, M.M.; Mykytyn, A.Z.; Breugem, T.I.; Wang, Y.; Wu, D.C.; Riesebosch, S.; van den Doel, P.B.; Schipper, D.; Bestebroer, T.; Wu, N.C.; et al. Human airway cells prevent SARS-CoV-2 multibasic cleavage site cell culture adaptation. *eLife* **2021**, *10*. [[CrossRef](#)]
33. Hee Ko, S.; Bayat Mokhtari, E.I.; Mudvari, P.; Stein, S.I.; Stringham, C.D.; Wagner, D.I.; Ramelli, S.; Ramos-Benitez, M.J.; Strich, J.R.; Davey, R.T.; et al. High-throughput, single-copy sequencing reveals SARS-CoV-2 spike variants coincident with mounting humoral immunity during acute COVID-19. *PLoS Pathog.* **2021**, *17*, e1009431. [[CrossRef](#)]
34. Johnson, B.A.; Xie, X.; Bailey, A.L.; Kalveram, B.; Lokugamage, K.G.; Muruato, A.; Zou, J.; Zhang, X.; Juelich, T.; Smith, J.K.; et al. Loss of furin cleavage site attenuates SARS-CoV-2 pathogenesis. *Nature* **2021**, *591*, 293–299. [[CrossRef](#)] [[PubMed](#)]
35. Klimstra, W.B.; Tilston-Lunel, N.L.; Nambulli, S.; Boslett, J.; McMillen, C.M.; Gilliland, T.; Dunn, M.D.; Sun, C.; Wheeler, S.E.; Wells, A.; et al. SARS-CoV-2 growth, furin-cleavage-site adaptation and neutralization using serum from acutely infected, hospitalized COVID-19 patients. *bioRxiv* **2020**. [[CrossRef](#)] [[PubMed](#)]
36. Rajah, M.M.; Hubert, M.; Bishop, E.; Saunders, N.; Robinot, R.; Grzelak, L.; Planas, D.; Dufloo, J.; Gellenoncourt, S.; Bongers, A.; et al. SARS-CoV-2 Alpha, Beta, and Delta variants display enhanced Spike-mediated syncytia formation. *EMBO J.* **2021**, *40*. [[CrossRef](#)]
37. Braun, K.M.; Moreno, G.K.; Halfmann, P.J.; Hodcroft, E.B.; Baker, D.A.; Boehm, E.C.; Weiler, A.M.; Haj, A.K.; Hatta, M.; Chiba, S.; et al. Transmission of SARS-CoV-2 in domestic cats imposes a narrow bottleneck. *PLoS Pathog.* **2021**, *17*, e1009373. [[CrossRef](#)]
38. Escalera, A.; Gonzalez-Reiche, A.S.; Aslam, S.; Mena, I.; Pearl, L.; Laporte, M.; Fossati, A.; Rathnasinghe, R.; Alshammery, H.; van de Guchte, A.; et al. SARS-CoV-2 variants of concern have acquired mutations associated with an 1 increased spike cleavage. *bioRxiv* **2021**. [[CrossRef](#)]
39. Kenney, S.P.; Wang, Q.; Vlasova, A.; Jung, K.; Saif, L. Naturally Occurring Animal Coronaviruses as Models for Studying Highly Pathogenic Human Coronaviral Disease. *Veter- Pathol.* **2020**, *58*, 438–452. [[CrossRef](#)] [[PubMed](#)]